Investigation of deformation pattern and sliding mode in dip slopes using discrete element method

Cheng-Han Lin[1], M.-C. Weng[2], and H.-H. Li[3]

[1] Department of Civil Engineering, National Cheng Kung University, Tainan City, Taiwan.
[2] Department of Civil Engineering, National Chiao Tung University, Hsinchu City, Taiwan.
[3] Chung Cheng Institute of Technology, National Defense University, Taoyuan City, Taiwan.

ABSTRACT

In the conventional Newmark sliding block method, permanent displacement develops along a single slip surface when a slope is subjected to a seismic motion that exceeds critical acceleration. However, for a slope with geological discontinuities, the Newmark approach could lead to an unsafe assessment that the plastic deformation may occur along the existing weak planes. In this study, the small-scale shaking table tests and the discrete element method were used to understand the dynamic responses of a slope with multiple weak planes under seismic condition. The effect of slope geometry and input motion property were explored. In addition, two types of sliding modes, namely differential and complete, were observed and could be distinguished by using the slope angle as the threshold. Compared to the Newmark approach, the numerical models exhibited greater permanent displacement at the slope crest than the theoretical estimation and the critical acceleration was greatly overestimated in all cases. The comparison indicates that sliding planes develop much more easily along existing discontinuities within the dip slope and can lead to even greater disasters than theoretical estimation by conventional Newmark approach.

Keywords: Dip slope; discrete element method; seismic-induced failure; sliding mode; shaking table test.

1 INTRODUCTION

In recent years, the earthquake occurred more frequently and triggered catastrophic landslides around the world. The failure of the dip slope, which contains multiple weak planes in the same dip angle along the slope face, is particularly notable when subjects to an external seismic loading. For example, in 1999 Chi-Chi earthquake, a huge rock block was released suddenly and sliding rapidly toward the down slope in Tsaoling, Nantou. The event caused sever loss of property and life. Therefore, the understanding of the failure mechanism and dynamic behavior is quite necessary for the hazard mitigation.

Several analytical methods have been developed to address the evaluation of slope stability under seismic condition. Jibson (2011) summarized these methods into three categories: (1) the pseudo-static method, (2) the sliding block method and (3) the stress-deformation method. Compared to the simple pseudo-static method and the complex stress-deformation method, the sliding-block method, which was introduced by Newmark (1965), is more practical for assessing the behavior of slopes during earthquake shaking. The Newmark approach assumed that the sliding mass above the slip surface is a rigid block. If the sliding block subjects to an excitation that exceeds the yield acceleration, the plastic deformation will develop along a single sliding plane. After the seismic loading, the slope exhibits a permanent displacement at the sliding plane. The yield acceleration is determined by employing seismic motion in the limit equilibrium analysis until the safety factor (FS) equals 1.0. Hence, the yield acceleration is often referred to as critical acceleration. The permanent displacement of the sliding block can be estimates by double integrating the parts of external excitation that exceed the critical acceleration. Based on the Newmark approach, the initiation of the slope failure induced by the earthquake can be assessed by the critical acceleration and the deformation behavior during the earthquake is evaluated by the permanent displacement.

Although the application of the Newmark approach on the practical engineering is simple and effective, its assumptions result in unsuitable to evaluate the stability of seismic-induced deep-seated landslides (Jibson, 2011; Gischig et al., 2015). In addition, the performance of the Newmark approach on the dip slope, which usually contains multiple weak planes inside the slope, remains unclear. Hence, this study conducted a series of small-scale shaking table tests and DEM simulations to investigate the dynamic responses of the dip slope during seismic loading. The influence of the slope geometries and the seismic motion properties were discussed in detail. Additionally, the critical acceleration and the permanent displacement were analyzed from the monitoring data of the tests. The performance of the Newmark approach was evaluated by comparing between analysis results and theoretical solutions. The physical tests and numerical simulations provided

insights on the seismic-induced dip slope failure and could contribute to the hazard mitigation associated with dip slopes.

2 METHODOLOGY

In this study, the small-scale shaking table test was first adopted to investigate the dynamic responses of the dip slope under the seismic condition. The model preparation followed the approach of Weng et al. (2017) in using the artificial rock ball as the basic material. The friction of the rock ball is 48.6° according to the result of the direct shear test. As shown in Fig. 1a, the dip slope model was constructed through the rock balls and placed on a single degree of freedom shaking table system. The system was driven by an MTS 244.21 servo-controlled hydraulic actuator, which can produce accurate and repeatable seismic motions to frequencies up to 12 Hz. A high-speed camera was placed in front of the shaking table to capture the real-time images. In addition, two accelerometers were stick on the shaking table (G1) and the top of the slope model (G2) for comparing.

The DEM software PFC2D was to understand the deformation pattern of the seismic-induced dip slope failure in detailed. In the DEM simulation, the particle element was used to construct the dip slope model. Because the particle element had the same geometry as the rock ball used in the physical tests, the results of two approaches were comparable and the DEM model could be verified according to the shaking table tests (Fig. 1b). The geometry of the DEM model is shown in Fig. 1c. In each computation interval, the acceleration, which is recorded by 12 monitoring points that were set on the right side of the model, can be calculated from the velocity changing. In the experiments and the simulations, the dip slope model was subjected to the sine harmonic wave from the base plate. This study designed the input motions with different PGA by controlling the frequency and the amplitude.

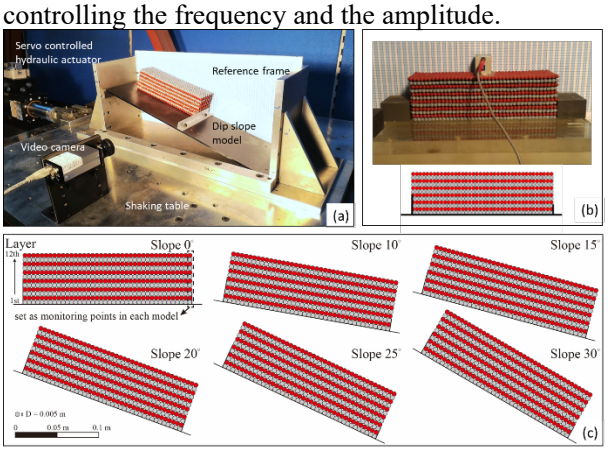

Fig. 1. Dip slope models of the shaking table test and the DEM simulation.

Table 1. Setting of the microscopic parameters of the DEM model.

Items		Value
Particle radius		2.50 x 10-3 (m)
Particle density		2650 (kg/m3)
Friction coefficient		0.70
Contact bond model	Normal stiffness	2.40 x 102 (N/m^3)
	Shear stiffness	1.00 x 102 (N/m^3)
Parallel bond model	Normal stiffness	5.00 x 108 (N/m^3)
	Shear stiffness	5.00 x 108 (N/m^3)
	Normal strength	1.00 x 105 (N/m^3)
	Shear strength	4.17 x 104 (N/m^3)

3 RESULTS

Figure 2a shows the deformation pattern of the dip slope model with 18 layers at the slope angle of 15° under the excitation of 0.48 *g*. Firstly, the deformation occurred at the top of the dip slope, and the permanent displacement increased during the deformation process. Two sliding planes developed at the top and toe of the model in the first second. In the next second, the dip slope continued moving downward along the deep sliding plane. The permanent deformation increased significantly and the mass above the sliding plane completely sliding toward downslope afterward. During the movement, the sliding mass remained complete in which no opening cracks were observed inside the model. In addition to the deformation process, the dynamic response of the slope model was recorded by the accelerometer mounted on top of the model. Figure 2b shows the acceleration variation compared with the PGA of the input excitation, which was recorded by the accelerometer set on the shaking table. Based on the monitoring, the motion of the dip slope mainly occurred between 0 to 3 seconds, and the model experienced its highest acceleration at about 1.5 seconds. To analyze the behavior of the seismic-induced dip slope failure, the critical acceleration was determined through the comparison between two accelerometers. As shown in Fig. 2b, when a sliding plane start to develop inside the slope, the acceleration recorded by G2 began to deviate from the record of G1. At this moment, the recorded acceleration of G2 was regarded as the critical acceleration of the dip slope model under seismic condition.

The results of the shaking table tests were then used to calibrate the setting of microscopic parameters of the DEM simulation. A normalized parameter δ/h, which is defined as the displacement of the right-edge particle divided by the slope height, was used to illustrate the characteristics of the slope model during the deformation. Figures 3a and 3b show the results of the 15° model under excitations of 0.32 *g* (frequency of 2 Hz and amplitude of 0.02 m) and 0.64 *g* (frequency of 4 Hz and amplitude of 0.01 m). Both models exhibited the rocking behavior at the first peak of the input motion, and the permanent deformation developed in the following excitation. In addition, the deformation was differential in each layer and two sliding planes were observed at the second and sixth layers. When the excitation end, the models subjected to accelerations of 0.32 *g* and 0.64 *g* had the greatest displacements of 0.03 m (50% of the model height) and 0.021 m (35% of the model height),

respectively. Figures 3c and 3d show that the 30° models moved along a major sliding plane and completely slid out under the input motions of 0.32 *g* and 0.64 *g*. The eventual displacements of the models under excitations of 0.32 *g* and 0.64 *g* were about 0.18 m (300% of the model height) and 0.3 m (500% of the model height), respectively. In general, the greatest displacement occurred at the top layer in response to the seismic loading due to the topographic effect. A strong positive correlation between the PGA of the input motion and the particle displacement was observed. In addition, the slope angle dominant the sliding behavior of the dip slope model.

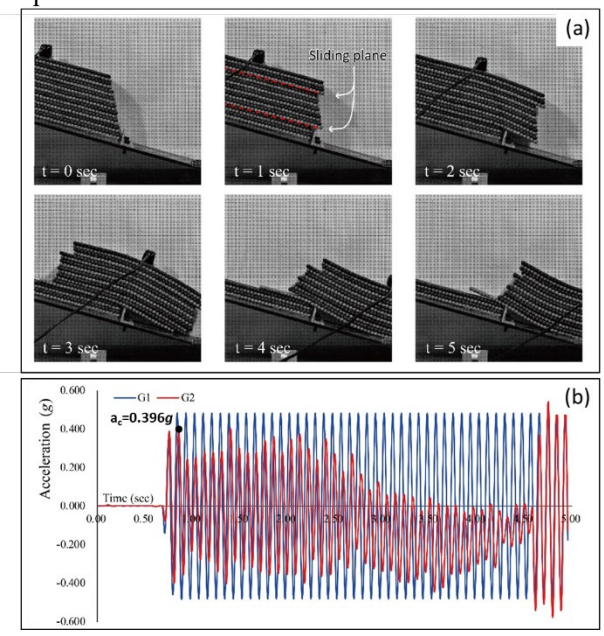

Fig. 2. Deformation pattern of the 15° model under the excitation of 0.48 *g*.

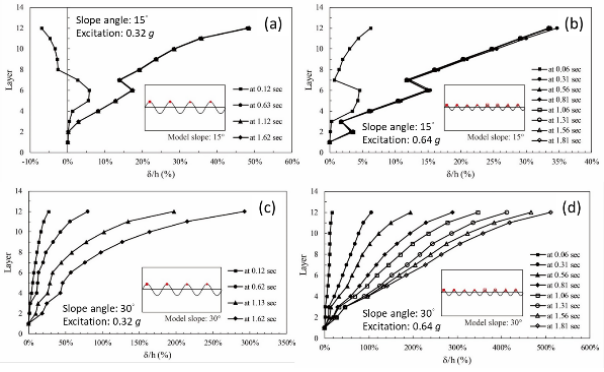

Fig. 3. Deformation process of the dip slope model during seismic loading.

4 DISCUSSIONS

4.1 Sliding modes of seismic-induced dip slope failure

Based on the shaking table tests and the DEM simulations, two types of the sliding modes, namely differential sliding and complete sliding, were observed for the dip slope under seismic condition. Figure 4 shows the deformation process of two failure types. For the 10° model, the plastic deformation slowly increased during the excitation, and the pattern of the dip slope exhibited differential deformation at the end of the seismic motion. The mass above the sliding planes remain on the slope but result in the presence of the permanent displacement inside the dip slope. On the other hand, for the 30° model, the deformation developed apparently and the rock sheets above the sliding planes completely slid out in the forepart of the excitation. In the case, most rock layers slid as one block and exhibited similar displacement. Accordingly, we considered that the slope angle could be used to determine the possible sliding mode of the seismic-induced dip slope failure. In this study, using the slope angle of 20° as the threshold of two types of failure modes was reasonable. Notably, the threshold of the slope angle could be influence by the friction angle of the pre-existing weak planes. In addition, for the simplification, the dip angle of the multiple weak planes and the slope angle were the same in this study; hence, the effect of the relationship between dipping and slope angle on the sliding modes requires further research.

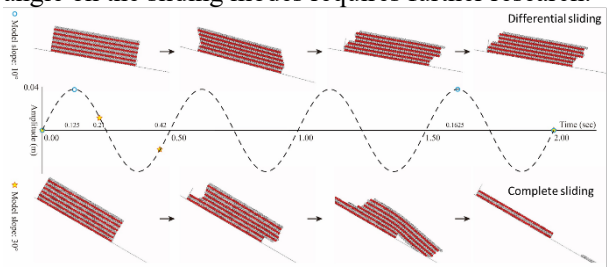

Fig. 4. Failure types of the dip slope under the seismic condition.

4.2 Comparison with Newmark sliding block analysis

Based on the shaking table tests and DEM simulations, this study evaluated the performance of the Newmark sliding block method on the failure of dip slope with multiple weak planes under seismic loading. Figure 5a shows the comparison of the critical acceleration between experimental results and theoretical solutions. Regardless of whether the vertical component of seismic loading was considered, the Newmark approach overestimated the critical acceleration in all cases. The difference between the shaking table tests and the Newmark approach increased when the slope angle decreased; moreover, the higher model was much easier to slide than the expectation of theoretical analysis due to the more existing weak planes. On the other hand, the permanent displacement of the DEM simulation was also compared with that of the Newmark approach (Fig. 5b). The comparison indicates that the theoretical solutions underestimated the permanent displacement in all models. The difference with the theoretical estimation increased under the seismic loading of low PGA. In addition, when the PGA of the seismic loading increased, the displacement inside the model increased significantly. Accordingly, for the dip slope under the seismic condition, the failure of the dip slope could occur earlier than the estimation of the conventional Newmark approach, and could lead to a

greater disaster because the deformation exceeds the expectation.

The key factor of the misestimation of the Newmark approach is that the presence of the existing weak planes is not considered by the conventional theoretical analysis. In the Newmark approach, the sliding mass above the sliding plane is simplified as a rigid block which neglects the effect of the pre-existing discontinuities under the seismic condition. In reality, the plastic deformation could develop along the geological discontinuities and result in the differential displacement and multiple sliding planes within the dip slope. Hence, the application of the Newmark sliding block method on assessing the stability of the dip slope under seismic condition may lead to the unsafe evaluation. The effect of the multiple weak planes should be considered for the analysis of the seismic-induced dip slope failure in the practical engineering.

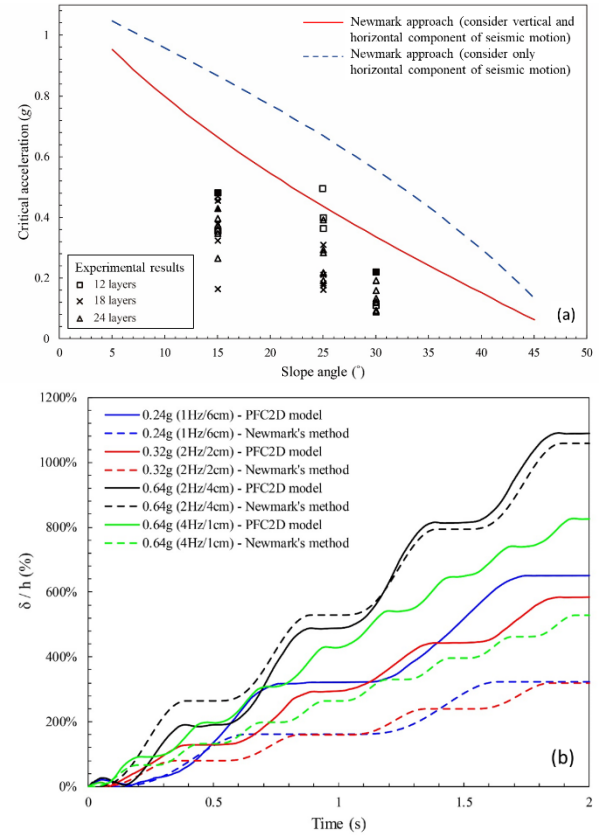

Fig. 5. Comparison of (a) the critical acceleration and (b) the permanent displacement between DEM simulations and Newmark method.

5 CONCLUSIONS

This study conducted a series of small-scale shaking table tests to investigate the dynamic behavior of the dip slope subjected to the seismic loading. By calibrating with the physical tests, the DEM simulations provided reasonable and considerable quantity of monitoring data to predict the dynamic responses of the dip slope under seismic condition. Two types of sliding modes, including complete sliding and differential sliding, were observed and could be distinguished by the angle of the inclined plane. In terms of the seismic motion, both frequency and amplitude affected the dynamic behavior of the dip slope, but they exhibited varying in-fluence degree on different sections of the dynamic behavior. In addition, increasing slope angle and slope height lead to amplify the dynamic responses of the dip slope. Compared with the Newmark approach, the critical acceleration and the permanent displacement during the seismic-induced dip slope deformation were misestimated by the theoretical analysis. The sliding planes could develop much easier along pre-existing weak planes within the dip slope and lead to even greater disasters than theoretical estimation by conventional Newmark approach. In this study, the performance of the DEM model was validated by the shaking table test. The future study could apply the DEM approach to analysis the real cases of the earthquake-induced landslide to provide recommendations for practice.

ACKNOWLEDGEMENTS

The authors would like to thank the Ministry of Science and Technology (Taiwan) for the supporting of research resources under Contracts MOST 104-2625-M-390-001, MOST 105-2625-M-390-001 and MOST 106-2625-M-390-001.

REFERENCES

Fan, G., Zhang, J.J., Wu, J.B., Yan, K.M. (2016). Dynamic response and dynamic failure mode of a weak intercalated rock slope using a shaking table. Rock Mech. Rock. Eng. 49, 3243–3256.

Gischig, V.S., Eberhardt, E., Moore, J.R., Hungr, O. (2015). On the seismic response of deep-seated rock slope instabilities—insights from numerical modeling. Eng Geol. 193:1–18.

Jibson, R.W. (2011). Methods for assessing the stability of slopes during earthquakes—a retrospec-tive. Eng. Geol. 122, 43–50.

Newmark, N.M. (1965). Effects of earthquakes on dams and embankments. Géotechnique. 15, 139–160.

Weng, M.C., Chen T.C., Tsai S.J. (2017). Modeling scale effects on consequent slope deformation by centrifuge model tests and the discrete element method. Landslides. 14:981–993.